Electronic Supplementary Material (ESI) for Analyst.
This journal is © The Royal Society of Chemistry 2022

Supporting information

A novel near-infrared fluorescent probe based on triphenylamine derivatives for rapid and sensitive detection of heparin

Mingming Liu, Jian Cao *, Cuiping Huang, Meijuan Zhang, Yanan Li, Chuanxiao Wang

School of Chemistry and Chemical Engineering, Shanghai University of Engineering Science, 333 Longteng Road, Shanghai, 201600, P. R. China Fax: 86-21-67791214

E-mail: caoj@sues.edu.cn

Contents

1. The photophysical properties of **TPA-P⁺**

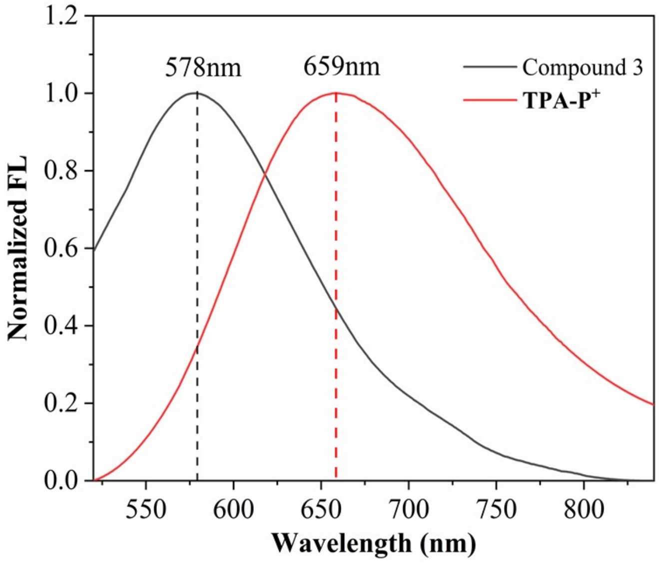

Figure S1.The fluorescence emission spectra of **TPA-P$^+$** and compound 3 in the water (containing 1% DMSO).

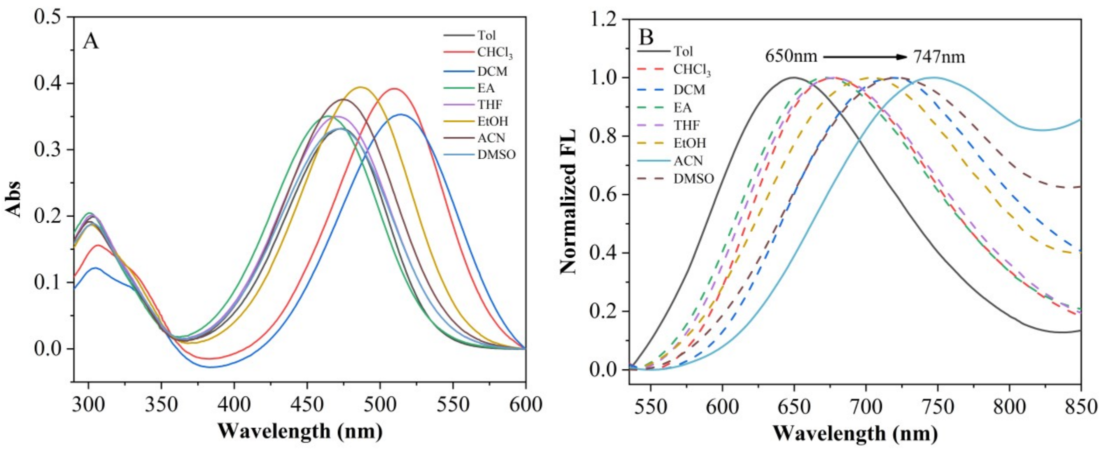

Figure S2. (A) Changes in absorption spectra and (B) Normalized fluorescence emission spectra of **TPA-P$^+$** (10 μM) in different solvents.

Table S1. Parameters of the solvents

solvent	Δf	λ_{abs}	λ_{em}	Stokes shift (cm^{-1})
Toluene	0.014	472	650	5802
$CHCl_3$	0.148	509	677	4875
DCM	0.217	514	720	5566
EA	0.221	464	672	6670
THF	0.21	471	677	6460
DMSO	0.263	472	721	7317
MeCN	0.305	474	745	7674
EtOH	0.29	486	706	6412

Δf was chosen as the measure of polarity. ε was the static dielectric constant and n was the optical refractive index of the solvent.

(1)

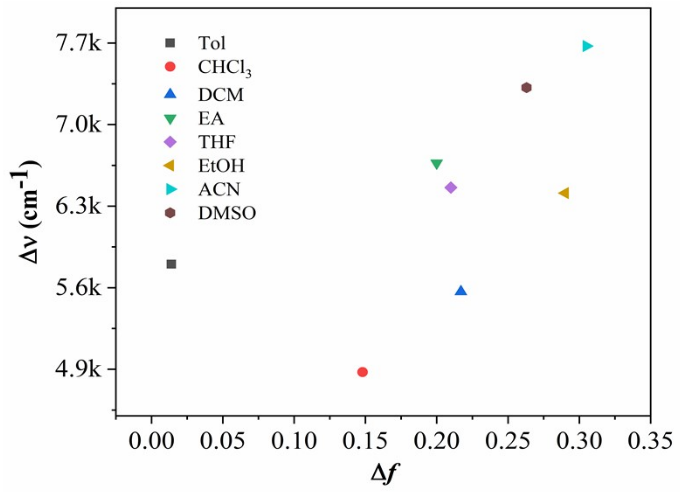

Figure S3. The Lippert-Mataga plot of Stokes shift (Δυ) of **TPA-P**$^+$ versus Δ*f* in different solvents.

2. DFT optimized structure of **TPA-P**$^+$

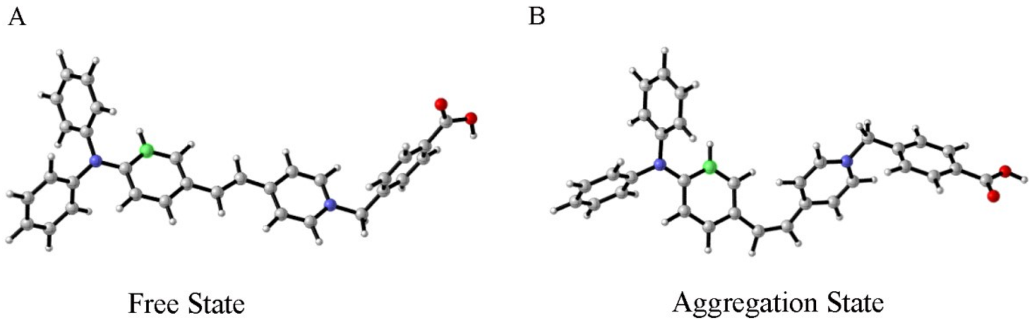

Figure S4. Density functional theory (DFT) optimized structure of **TPA-P**$^+$. In the ball-and-stick representation, hydrogen, carbon, nitrogen and oxygen are colored in white, gray, blue and green, red, respectively. The calculations are based on the optimized ground state geometry (S_0 state) at the B3LYP/6-31g*/ level using Gaussian 09W.

3. The response of compound 3 to heparin

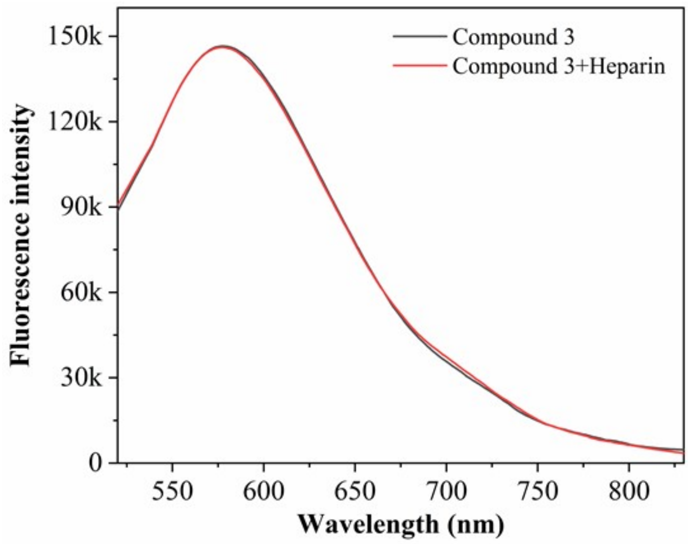

Figure S5. The response of compound 3 to heparin.

4. Stability of free **TPA−P⁺** and **TPA−P⁺**+heparin complex

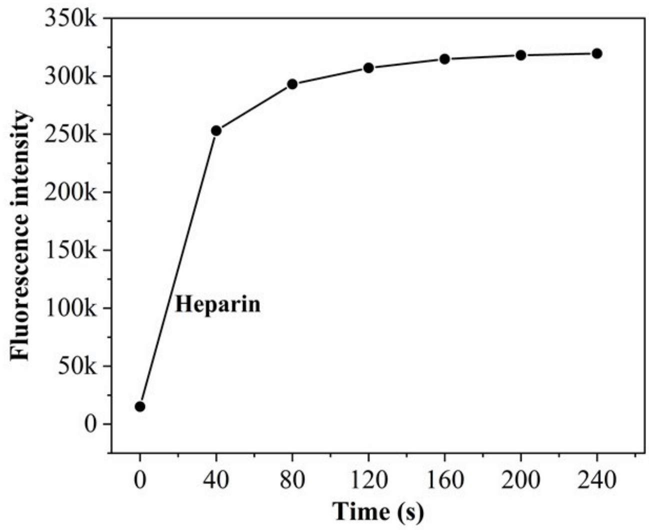

Figure S6. Time response of **TPA-P**$^+$ (2.5 μM) to heparin (2.0 nM) in the water (containing 1% DMSO).

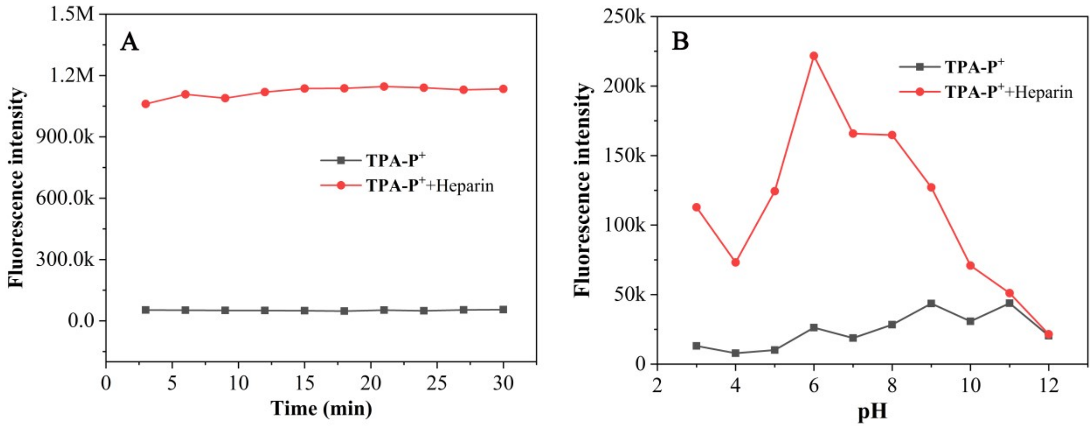

Figure S7. Effect of time (A) and pH (B) on free **TPA-P**$^{+}$ and **TPA-P**$^{+}$+heparin complex in the water (containing 1% DMSO). λ_{ex} = 470 nm

5. The selectivity of **TPA−P**$^{+}$+heparin complex to PRTM

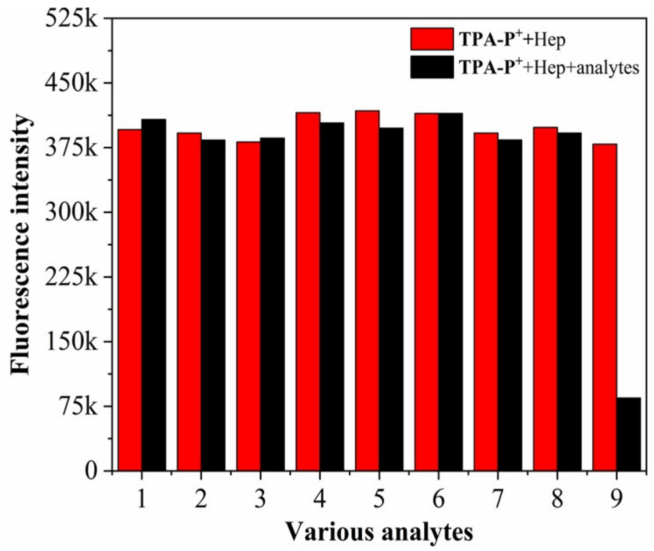

Figure S8. Selectivity of **TPA−P**$^{+}$+Heparin complex for sensing of PRTM over other possible analytes including:1Valine (Val); 2 Histidine (His); 3 Glutathione (GSH); 4 Cystine (Cys); 5 Serine (Ser); 6 Tryptophen (Try); 7 NaCl; 8 KBr; 9 Protamine (PRTM). λ_{ex} = 470 nm

6. Reversibility of the "off-on-off" system constructed by **TPA−P**$^{+}$+heparin+PRTM

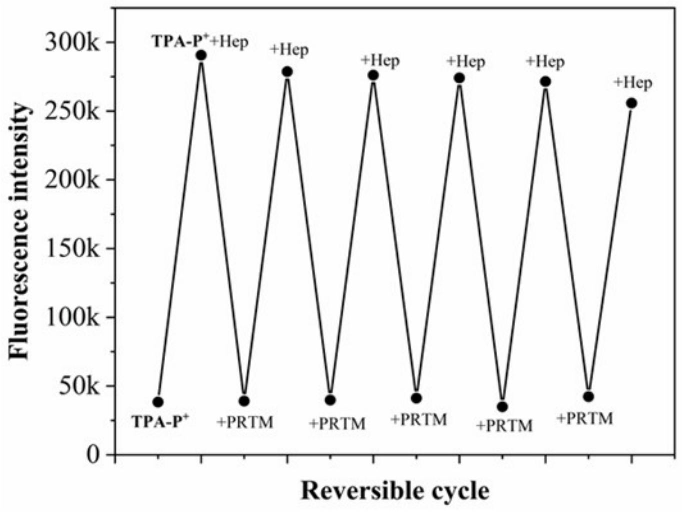

Figure S9. Reversibility of **TPA-P+** (5.0 μM) in subsequent response to heparin (10 μg/mL) and PRTM (15 μg/mL) in the water (containing 1% DMSO). λ_{ex} = 470 nm.

7. Heparin sensing in serum containing 100 μM NaCl

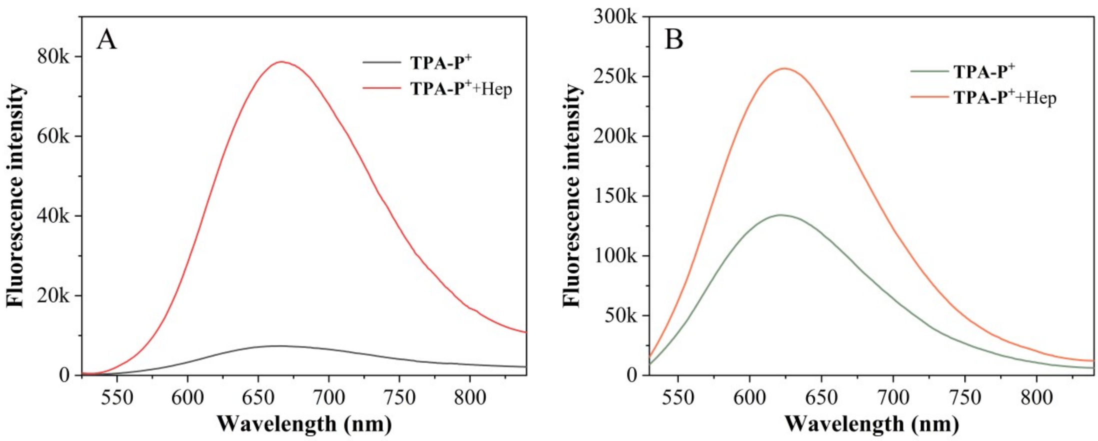

Figure S10. After adding 100 μM NaCl, emission spectral changes of **TPA-P+** (2.5 μM) upon addition of heparin (16 μg/mL) in water (A) and human serum (B) (containing 1% DMSO)

8. HRMS and NMR characterizations

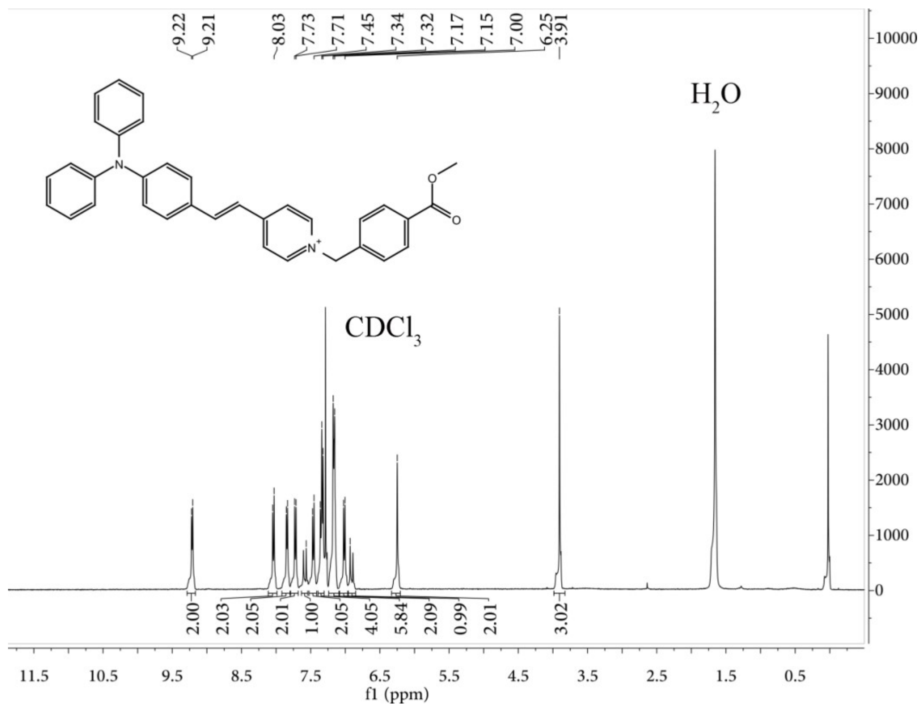

Figure S11. The ^{1}H NMR spectra of **TPA-P$^+$** in $CDCl_3$.

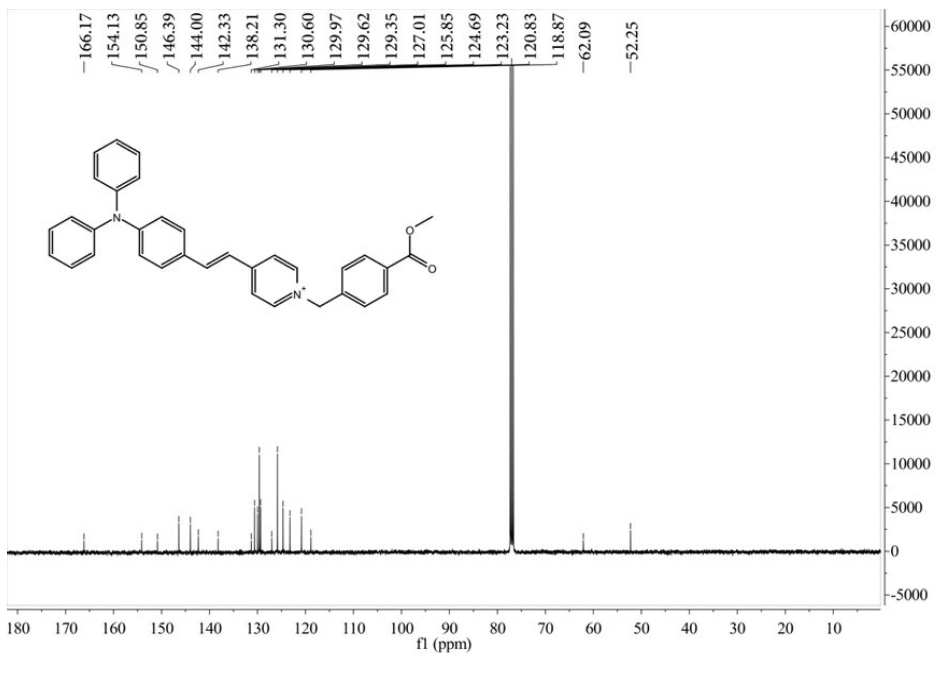

Figure S12. The ^{1}C NMR spectra of **TPA-P$^+$** in $CDCl_3$.

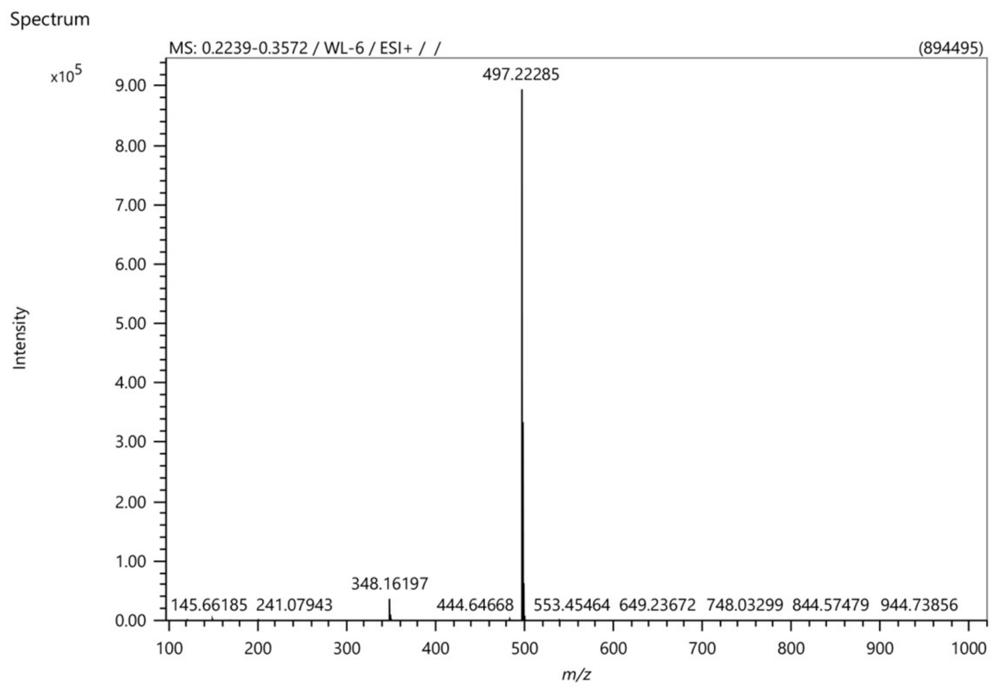

Figure S13. The HRMS spectra of **TPA-P$^+$**.